J Solid State Electrochem (2008) 12:1421–1434
DOI 10.1007/s10008-007-0494-y

ORIGINAL PAPER

How to affect number, size, and location of metal particles deposited in conducting polymer layers

V. Tsakova

Received: 30 August 2007 / Revised: 7 November 2007 / Accepted: 3 December 2007 / Published online: 9 January 2008

Abstract This paper presents a review on a series of recent investigations focused on the understanding of the role of various factors for the number, size, and location of the metal particles electrodeposited in conducting polymer (CP) layers. It is demonstrated that the initial oxidation state of the CP layer and its surface and bulk structure play an important role for the location of the metal particles. The use of metal anion complexes instead of the corresponding metal cations presents a helpful tool for affecting the location and number of metal crystals. The involvement of special metal/polymer interactions in the metal electrocrystallization process is another way for influencing the metal deposit. An alternative to the electrodriven deposition is the electroless metal precipitation based on the reducing ability of the CP layers. This approach results in metal particles deposition at the polymer surface and may be effectively controlled through parameters such as CP reduction charge, dipping time, and concentration of the metal-plating solution.

Keywords Conducting polymers · Metal electrodeposition · Electroless precipitation · Cu · Ag

Introduction

Since the early works of Tourillon and Garnier [1] and Chandler and Pletcher [2] published in the mid-1980s, a number of investigations were focused on metal electrodeposition in conducting polymer (CP) materials. A great number of studies were directed to metal/polymer systems of practical interest and several metals such as Pt [1–43], Pd [2, 14, 22, 44–51], Ag [1, 52–56], Au [57–62], Cu [48, 52, 63–76], Ni [52, 77–80], Pb [2, 28, 52], etc. were addressed. Table 1 summarizes the publications on metal particles electrodeposition in the most studied CPs—polyaniline (PANI), polypyrole (PPY), polythiophene (PTHI), and poly-3,4-ethylenedioxythiophene (PEDOT). Despite the numerous studies and the continuing interest in the field, most of the works describe metal electrodeposition in polymer layers with various and, in some cases, ill-specified characteristics, and thus do not provide the basis for comparison between results obtained at different experimental conditions. Therefore, it is difficult to gain a general understanding on the possibilities for influencing the characteristics of the metal deposit such as number, size, and spatial distribution of the electrodeposited metal crystals.

This was the reason for performing a series of investigations [82–95] under well-defined conditions aimed at probing different approaches for metal particles electrodeposition. The basic goal was to identify factors providing the opportunity to influence, in a controlled way, the type of the metal deposit. The choice of metals in these investigations was not determined from an application point of view but rather from the point of view of screening different situations with respect to the intrinsic properties of the CP materials. Thus, we started by studying copper [82–84, 86–88] and silver [53, 89, 90] deposition in PANI layers; these two particular metals having equilibrium potentials, which are negative and correspondingly positive with respect to the main redox peak of PANI (Fig. 1). Copper and silver also provide the opportunity to compare deposition using metal cations (Cu^{2+} or Ag^{+}) and a variety of metal anion complexes.

In parallel with studies on metal electrocrystallization in PANI and also in the ring-substituted poly-*o*-methoxyaniline

V. Tsakova (✉)
Institute of Physical Chemistry, Bulgarian Academy of Sciences, Sofia, Bulgaria
e-mail: tsakova@ipc.bas.bg

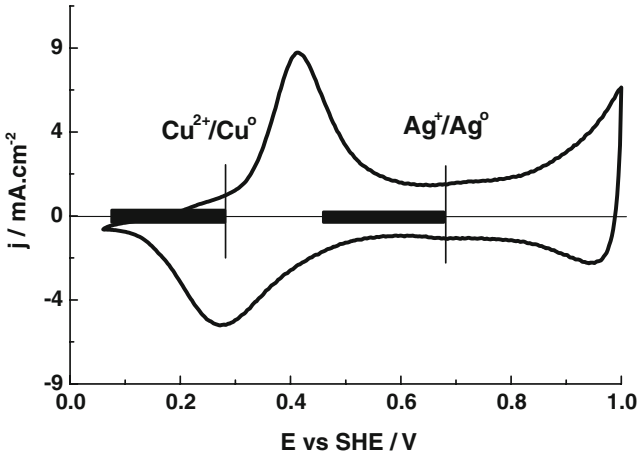

Fig. 1 Voltammetric curve of PANI measured in acid solution (0.5 M H_2SO_4); v=100 mVs^{-1}

(POMA) [94], investigations on palladium and copper deposition in PEDOT [85, 91–93, 95] were started. Although with very different equilibrium potentials, both metals deposit in potential windows where PEDOT is in its oxidized, high-conducting state. Nevertheless, the situation for both metals turned out to be drastically different because of an important peculiarity concerning copper electroreduction in PEDOT. It was found that under specific conditions copper becomes stabilized by the bulk of the PEDOT layer [91, 92], and this process may be used to influence the copper electrocrystallization [93].

Finally, a series of experiments was performed to study the chemical, electroless precipitation of metal particles in PANI [90] and PEDOT [95]. The term electroless precipitation is used to differentiate this CP-based process from the conventional electroless deposition; the latter requiring an additional reducing agent present in the electrolyte solution. Electroless precipitation occurs by coupling polymer oxidation and metal ions reduction. This approach, initially studied for the recovery of precious metals from acidic solutions [96–101], has been in the meantime often employed for intentional deposition of metal particles in CP layers [50, 102–127] (Table 1).

The present review aims at outlining some of the most important results obtained in our studies and pointing to factors allowing for a significant change in the microscopic picture of the metal deposit. Each of the following parts in this review addresses a separate issue and presents examples in various metal/CP systems originating from both our investigations and other relevant publications in the field.

Experimental

PANI and POMA layers were synthesized in 0.1 M monomer solution in sulfuric acid (0.5 M) by means of three different experimental techniques—potentiostatic, potentiodynamic, and pulse potentiostatic deposition [83]. The pulse potentiostatic procedure [128, 129] consisted of a sequence of consecutive polymerization (E=1.0 V) and reduction (E=0.2 V) pulses with equal duration (0.1 s). Chemical synthesis of PANI on supporting platinum plate was carried out in 0.01 M aniline, 0.01 M $(NH_4)_2S_2O_8$, and 0.5 M H_2SO_4 at 4 °C under constant stirring [88]. PEDOT layers were synthesized potentiostatically using an aqueous microemulsion containing 0.068 M monomer, 0.5 M $LiClO_4$, and 0.04 M poly-oxyethylene-10-lauryl ether (Sigma) as surfactant [130, 131]. The working electrodes used throughout most of the electrochemical measurements were single crystal platinum beads embedded into glass with surface area between 2×10^{-3} and 2×10^{-2} cm^2. Specimens for SEM were obtained by using platinum plate electrodes. As an indirect measure for the thickness of PANI and POMA layers, we used the reduction charge, Q_{red}, obtained after electrochemical synthesis by cyclic voltammetry performed in 0.5 M H_2SO_4. This charge is an easily measurable characteristic of the layer providing the opportunity to control the thickness of the polymer coating. A reference measurement of the thickness of a PANI layer was carried out through SEM using a scratched surface and served for rough estimate of the PANI layer thicknesses on a 20 $mCcm^{-2}$ reduction charge per 1 μm basis. In the case of PEDOT, the thickness of the layers was estimated by measuring the polymerization charge obtained in the course of potentiostatic polymerization.

Copper deposition was studied by using three different solutions: (1) 0.033 M $CuSO_4$ and 0.5 M H_2SO_4 (copper cations solution); (2) 0.02 M $CuSO_4$, 0.062 $K_3C_6H_5O_7$, and 0.344 M K_2SO_4, pH 6.06, (copper citrate solution) [86]; (3) 0.02 M $CuSO_4$, 0.06 M $Na_2C_2O_4$, and 0.344 K_2SO_4, pH 6.5, (copper oxalate solution) [87]. In all cases, copper was deposited galvanostatically at j=−0.17 mA cm^{-2}. The amount of deposited copper was varied by carrying out the galvanostatic experiment for different times, typically in the range between 200 and 600 s.

Silver deposition was carried out also in three different solutions: (1) 0.01 M $AgClO_4$ and 0.5 M $HClO_4$ (silver cations solution); (2) 0.01 M $AgNO_3$, 0.04 M $Na_2S_2O_3$, and 0.5 M KNO_3, pH 6.4, (Ag–thiosulfate solution); (3) 0.4, 2, or 10 mM $AgNO_3$, 0.02 M $Na_2C_{10}H_{14}O_8N_2$ (disodium salt of ethylenediaminetetraacetic acid [EDTA]), 0.5 M KNO_3, pH 4.1, (Ag–EDTA solution) [90].

Palladium deposition in PEDOT was studied in 2 mM $PdSO_4$ in 0.5 M H_2SO_4 by means of potentiostatic experiments [85, 95] and electroless precipitation [95].

In some sets of experiments on the role of the initial oxidation state of the CP layer and also in the case of electroless precipitation, PANI and POMA layers were subjected to reduction in indifferent electrolyte (0.5 M

Table 1 Investigations on metal particles deposition in the most studied CPs

Metal	PANI[a]	PPY[a]	PTHI[a]	PEDOT
Metal particles electrodeposition				
Pt	3, 6, 7, 9, 12, 13, 15, 16–19, 20, 22, 23, 25–27, 30, 31, 32–35, 39, 40, 43	2, 3, 5, 8, 9, 20, 21, 24, 36, 41	1, 14, 20, 28	37, 38, 42
Pd	22, 46, 47, 49–51	2, 45, 46, 48	14, 44, 48	85, 95
Au	57, 59–62	58		
Ag	53, 55, 56, 89, 90	52	1	
Cu	66, 70, 82–84, 86, 87, 94	48, 52, 64, 67, 69, 71, 72–76	48, 65, 68	63, 71, 91–93, 95
Ni	78	52, 67, 71,79, 80	77	71
Other metals	Cd: 66	Ir, Ru: 41, Sn: 52, Pb: 2, 52, Co: 81, 159, Fe: 159, Ni: 159	Rh: 14, Pb: 28	Co: 71
Bimetal deposition	Pt–Ru: 11, 19, 29, 31, 40, Pt–Sn: 11, 19, Pt–Pb: 19, 20, Pt–Os: 31, Pt–Mo: 31	Pt–Pb: 20, Co–Gd: 71, Fe–Ni: 159, Co–Mn: 159	Pt–Sn:10, Pt–Pb:20	Pd–Cu: 95, Co–Gd: 71
Metal electroless precipitation				
Pt	125, 127			
Pd	101, 104, 106–111, 113, 115, 118, 120	112		95
Au	96, 97, 98, 113, 117, 127	98, 114		114, 116, 119
Ag	90, 100, 103, 123, 127	99, 122, 123, 126	105	126
Other metals	Hg: 102, 124			
Incorporation of chemically synthesized metal nanoparticles				
Pt	156	24, 36, 153, 154		
Pd	151	155		
Metal/CP interactions				
Pd	106, 120, 150, 151			
Au		139		
Ag	103			
Cu	152	140–143	144–149	91, 92

[a] Derivatives of PANI, PPY, and PTHI are also included in the respective columns.

H_2SO_4) by keeping the potential at E=0.02 V for 15 min. Electroless precipitation in PEDOT was carried out after reducing the layers at E=−0.05 V for 1,200 s in sulfuric acid solution. (All potentials are quoted with respect to SHE.)

Electrodeposition of metal particles

Role of the initial oxidation state of the polymer layer

It is well known that the conductivity of the CP materials depends on their oxidation state, which in turn is potential- and, in some cases, pH-dependent. The conductivity of the polymer layer is, however, only one of the characteristics important for metal particles deposition. The second basic characteristic involved in the metal deposition process relates to the CP porous structure providing the opportunity for the transport of ions into the bulk of the layer down to the underlying metal electrode surface. Thus, there is always a competition between the reduction of metal ions on the outer and/or inner polymer surface and on the underlying metal surface. The outcome of this competition depends on the specific combination of morphology and conducting properties occurring under given experimental conditions.

An example illustrating this situation provides the Cu/PANI system. Due to the specific position of the equilibrium potential of Cu^{2+}/Cu with respect to the main PANI redox peak (Fig. 1), copper electroreduction in these CP layers may be initiated in two ways—either by taking the PANI layer in the oxidized, high-conducting state or by first reducing the layer and then starting the metal deposition in the reduced, low-conducting state of PANI. Figure 2 shows the galvanostatic transients obtained in the presence of copper ions in the electrolyte solution at PANI layers with one and the same thickness, the only difference being the initial oxidation state of PANI. It is evident that after the partial reduction of the PANI layer, electroreduction of copper started easily in the ox-PANI case and proceeded at potentials close to equilibrium. In contrast, copper nucleation and growth in the red-PANI case required high overpotentials and was obviously significantly inhibited.

Investigation on copper dissolution (Fig. 3), performed after the deposition in both cases, showed that the Cu oxidation peaks were markedly shifted. Copper deposited in

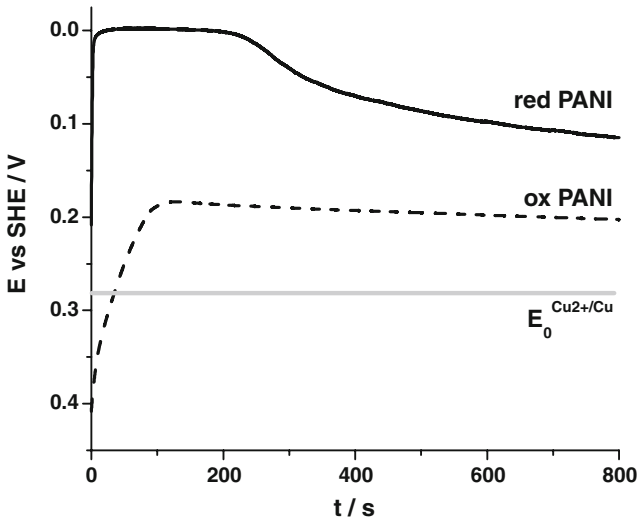

Fig. 2 Galvanostatic transients obtained in 0.5 M H_2SO_4+0.033 M $CuSO_4$ at an oxidized and a reduced PANI layer; j=−0.17 mAcm^{-2}, Q_{red}=20 mCcm^{-2}

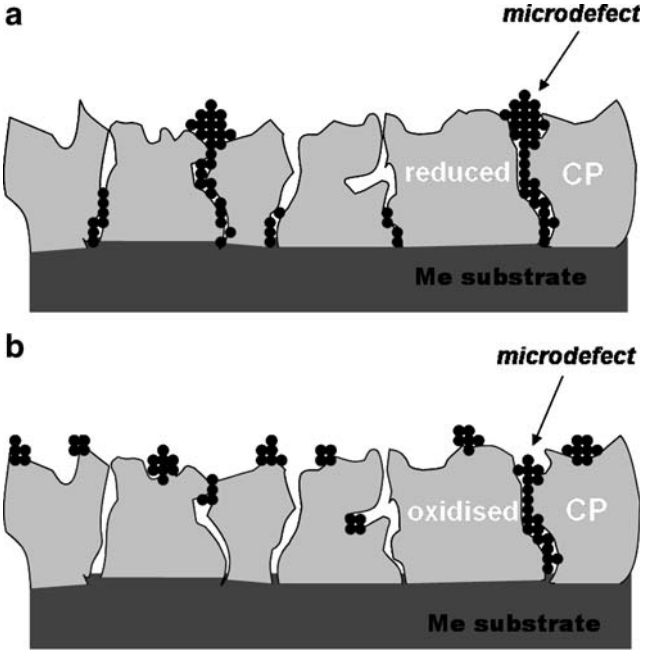

Fig. 4 Model for metal particles deposition in reduced (**a**) and oxidized (**b**) CP layer

the red-PANI layer became oxidized at more positive potentials, only after the oxidation transition of the PANI layer itself was initiated. Combined electrochemical and XPS experiments [84] have shown that copper dissolving under the second, more positive oxidation peak is located inside the polymer layer. No copper clusters were detected on the PANI external surface when small amounts of copper were electrodeposited in reduced defect-free PANI layers [88], indicating the presence of copper clusters inside the polymer structure. (The role of microdefects for the metal nucleation in CPs will be addressed further below.) Based on the electrochemical, XPS, and SEM results obtained in our studies, it was assumed that electrocrystallization in reduced and homogeneous PANI layers occurs by diffusion of the metal ions through the porous structure

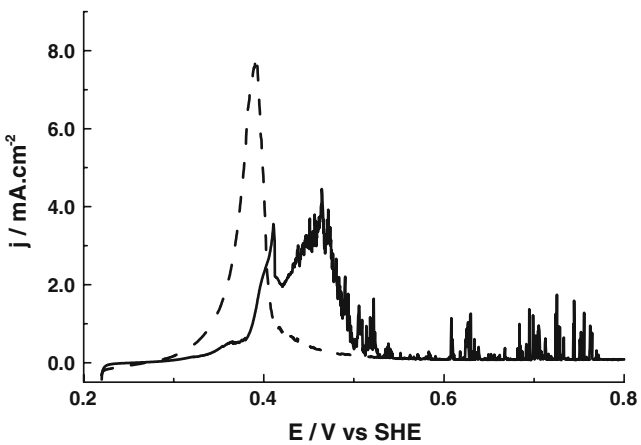

Fig. 3 Copper oxidation curves measured in 0.5 M H_2SO_4 at v= 5 mVs^{-1} after galvanostatic deposition in reduced (*solid lines*) and oxidized (*dash-dot lines*) PANI layers

of the polymer layer and formation of metal nuclei at the substrate/polymer interface (Fig. 4a). Further highly impeded growth due to the inhibited diffusion and the resulting low effective ions concentration proceeds through the polymer pores up to the polymer/solution interface. Thus, a network of fine metallic wires filling the porous structure is very probably created. After reaching the polymer/solution interface, the metallic caps will grow much easier due to the availability of enough metal ionic species. However, it could be argued that because of the very different growth rates of metallic wires inside the polymer and of metal caps already emerging at the polymer surface, the latter will gradually consume the whole diffusive flux and thus limit the growth of the still undergrown metallic wires. On the other hand, electrocrystallization performed at an oxidized, high-conducting PANI layer with a good surface homogeneity should preferentially occur at the polymer surface (Fig. 4b). The diffusion of ions inside the layer is impeded by the consumption of the ions flux at the surface, and the porous structure imposing transport limitations is of little importance for the metal nucleation process. Figure 4a and b is distorted in what concerns the size scale of layer thickness (several micrometers) and pore diameters (several nanometers [132]. The so-called microdefects correspond to the largest pores and have diameters from several hundreds of nanometers [132].

According to Fig. 2, there is a marked difference in the growth overpotential for copper clusters built in reduced and oxidized PANI layers. Therefore, it should be expected

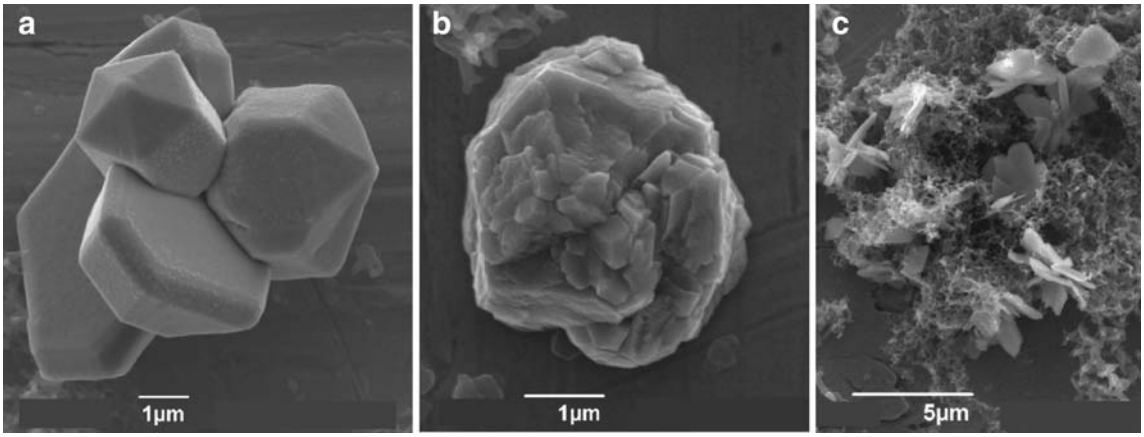

Fig. 5 SEM of copper crystals obtained by galvanostatic deposition of Cu at oxidized (**a**, **c**) and reduced (**b**) PANI layers. Copper crystals interlocked in loose surface PANI formations (**c**) are observed only in oxidized PANI; j=−0.17 mAcm^{-2}, Q_{red}=20 mCcm^{-2}

that the growth shapes of the crystals will depend on the initial oxidation state of the PANI layer. The SEM micrographs shown in Fig. 5a and b demonstrate this difference for the biggest Cu crystals observed at the PANI surface and show the formation of pentagonal copper crystals deposited at low overpotential (in an oxidized PANI layer) and the building of highly disordered copper clusters deposited at high overpotential (in a reduced PANI layer). Pentagonal copper crystals with different shapes were already observed in studies on copper electrocrystallization on titanium nitrate and copper polycrystalline substrates [133, 134]. Only in the case of electrodeposition in the oxidized state of PANI copper lamellar crystal, interlocked in the polymer structure (Fig. 5c), were found on the surface.

The above-suggested model for electrodeposition in oxidized and reduced CP layers is supported by the investigations of Yang and Wen [18] on the potentiostatic electrodeposition of platinum in PANI. The experiments were carried out at two outermost potentials (shifted by 400 mV) corresponding to the oxidized and reduced state of the polymer layer, respectively. Auger depth profiles showed preferential Pt deposition at (and close to) the polymer/electrolyte interface for the oxidized PANI layer and homogeneous distribution of platinum inside the reduced PANI structure [18].

Surface morphology and bulk structure of the CP layer

The discussion on the role of the CP oxidation state presented above is based on a model picture corresponding to a more or less ideal situation of a completely homogeneous (at the micrometer scale), defect-free polymer surface. It is known that the extent of the polymer homogeneity depends on several parameters, e.g., CP layer thickness, electrochemical polymerization procedure (potentiostatic, galvanostatic, potentiodynamic, pulse potentiostatic, etc.), and synthesis method (chemical or electrochemical). Thin CP layers are often highly defective and ill-reproducible in their micromorphology. Thus, it is difficult to study the metal nucleation and growth process and to differentiate between the role of the metal substrate and of the polymer coating for the electrochemical nucleation. Because of the multiple parameters influencing the polymer layer growth and structure, the only way to find out the thickness corresponding to a homogeneous CP layer of a given type seems to be microscopic imaging of the surface. In fact, the inhomogeneity of the polymer layer seems to be in the origin of the building of metal particles with sizes in very different scales (e.g., nanometer-sized and micrometer-sized) simultaneously observed on the polymer surface. The role of the microdefects and thickness of the CP layers for the electrochemical nucleation and growth of metal particles was extensively studied in our investigations on Cu deposition in PANI [83, 84, 88] and POMA [94] and Ag deposition in PANI [89].

By means of combined SEM and electrochemical experiments and by using copper electrocrystallization for decoration of the microdefects in the polymer layer, we have studied the amount of microdefects in PANI layers synthesized through potentiostatic, potentiodynamic, or pulse potentiostatic experiments [83]. The observation of metal crystals at two different size scales allowed identifying the microdefects in the polymer structure. It was established that the largest amount of defects (5×10^5 cm^{-2}) was found in potentiostatically synthesized PANI, whereas using the pulse potentiostatic procedure resulted in the lowest amount of microdefects (2.6×10^4 cm^{-2}) in the PANI structure.

In our investigations on Ag deposition in PANI [89], it was found that for thin PANI layers with thickness below 0.3 μm, the electrodriven metal nucleation occurred on the underlying metal surface through defects in the polymer structure. For thicker PANI layers exceeding the 0.3 μm thickness limit, the microdefects seemed to be leveled out

and the silver crystals were formed preferentially at the polymer/electrolyte interface.

Some elucidating results were obtained by comparing chemically and electrochemically synthesized PANI layers [88]. Although in both cases the obtained surface structure was homogeneous at the microscopic level, the chemically synthesized layers showed a rough surface with looser structure whereas the electrochemically synthesized PANI layers had a compact globular surface morphology. This difference in surface structure resulted in a marked difference with respect to the metal electrodeposition. The chemically synthesized coatings allowed for an easy deposition of equally sized copper crystals. The number of crystals did not depend on the thickness of the PANI layer except for very thin layers having microdefects. In contrast, the copper deposition in electrochemically synthesized PANI coatings was highly inhibited and resulted in the formation of crystals with broad size distribution [83, 84]. The number and size distribution of the metal crystals in the latter case depended markedly on the PANI layer thickness.

Another example illustrating the role of both layer thickness and surface structure provides the Cu/POMA system [94]. It was found that for thin POMA layers (<1 μm), irrespective of the electrosynthesis procedure (potentiostatic, potentiodynamic, or pulse potentiostatic), copper deposition proceeded in one and the same way through the polymer porous structure (Fig. 6, gray lines). For much thicker POMA layers (>1 μm), a marked difference was found in the surface structure, depending on the electrosynthesis procedure: a compact structure characterized POMA layers synthesized through potentiodynamic cycling or potentiostatic pulses while a much rougher surface structure was observed for POMA synthesized in the potentiostatic way [94]. Apart from this effect, there was also a marked difference in the initial reductive behavior of the thick POMA layers (Fig. 6, black lines). As a consequence, two different scenarios for copper nucleation and growth seemed to operate: for POMA layers with compact morphology remaining reduced in the course of deposition (e.g., potentiodynamically synthesized POMA), metal nucleation occurred most probably by impeded transport of the metal ions through the polymer microporous structure, possibly at the underlying metal surface (Fig. 4a). On the other hand, a larger extent of oxidation of the POMA chains and a rough surface structure (as is the case of potentiostatic POMA) resulted most probably in preferential metal deposition on available conducting polymer chains in the polymer structure.

A further example on the role of the CP surface structure for the metal electrodeposition may be found in the studies on Pt deposition in PANI [34]. The surface structure of the PANI layers was influenced by using two different polymer electrosynthesis procedures—galvanostatic and pulse galvanostatic, resulting in granular and fibrilar morphologies of the layers, respectively. In both cases, Pt particles with size varying between 100 and 400 nm were observed; the fibrilar, looser structure, however, offering a larger internal surface for the deposition [34].

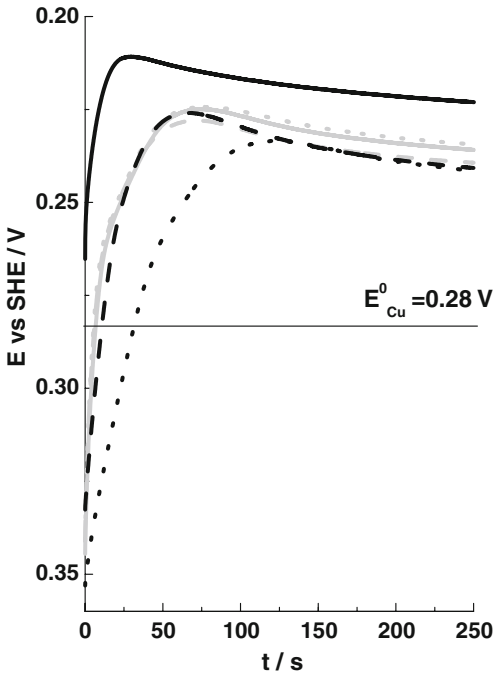

Fig. 6 Galvanostatic reduction curves obtained in 0.5 M H_2SO_4+ 0.033 M $CuSO_4$ at Q_{red}=22 mCcm^{-2} (*thin*, *gray lines*) and Q_{red}= 87 mCcm^{-2} (*thick*, *black lines*) POMA layers synthesized at constant potential (*dot lines*), by cyclic voltammetry (*solid lines*) and by potentiostatic pulses (*dash-dot lines*)

A comparative study demonstrating the role of the surface structure of PANI layers for Pd particles electrodeposition was recently published by Mourato et al. [51]. Pd particles were potentiostatically deposited from sulfate solution in PANI layers differing in their surface morphology and thickness. The AFM observations, carried out after long-time potentiostatic experiments, revealed the presence of nanometer-sized (50–90 nm) particles with relatively narrow size distribution located on top of the PANI layer with the more compact surface structure. The use of layers with a rougher porous structure resulted in Pd particles with larger size distribution (50–180 nm) located on the globular PANI surface. Possible formation of metal clusters inside the polymer matrix was also suggested in the latter case [51].

Source for metal reduction—metal anion complexes vs metal cations

The involvement of metal anion complexes instead of the corresponding metal cation in metal electrocrystallization is a well-known approach in the practice of galvanic electroplating used for improving the characteristics of the metal

coatings. Metal anion complexes are necessarily used for the electrodeposition of metals such as Pt, Au, Ir, and Pd (from chloride solutions). The special role of metal anion complexes for the electrodeposition in CPs consists in the possibility to involve them in the doping of the CP materials (by replacing the preexisting anions or by polymer synthesis in presence of these species). The different electrodeposition techniques exploiting this possibility are discussed further in the "Metal stabilization in CPs as a preliminary step for metal electrocrystallization" section.

There are few works dealing with anion complexes of metals, which are otherwise typically used as cationic species, e.g., silver thiocyanide for Ag electrodeposition in PANI [54] and copper and nickel oxalates for Cu and Ni electrodeposition in functionalized PPY [69, 80], none of them providing comparison with the corresponding metal cations deposition case.

In a series of studies [86, 87, 90], we have compared copper and silver electrodeposition in PANI using different complex anions of Cu and Ag without allowing for preliminary exchange of the doping anion in the CP material.

In the case of copper deposition, electroreduction was performed by using Cu–citrate [86] and Cu–oxalate [87] anion complexes. Figure 7a shows the galvanostatic transients obtained during electroreduction in three copper-containing (Cu^{2+}, Cu–citrate, and Cu–oxalate) electrolytes at PANI layers synthesized under one and the same conditions and having equal reduction charge. As expected, the use of copper anion complexes shifted the potential window for metal deposition in the negative direction in comparison to the corresponding cation. The galvanostatic curves obtained in these experiments reflected the involvement of several reduction reactions—reduction of metal ions, reduction of the CP layer itself, and also hydrogen reduction (for the Cu^{2+} case). This complicated situation impeded the attempts for quantitative interpretation of the galvanostatic curves. Nevertheless, the comparison of galvanostatic measurements in the presence and absence of the metal anion complexes indicated qualitatively to the following [86, 87]: The sharp maximum observed in the Cu–oxalate case (Fig. 7a) gave evidence for a dominating process of metal nucleation and growth with expanding surface of the growing metal phase [135–138], although measurements in supporting electrolyte showed that copper and PANI reduction proceeded in this case in parallel. The galvanostatic curve, obtained in the Cu–citrate case (Fig. 7a), showed inhibited metal nucleation and growth proceeding in a completely reduced CP layer at high overpotentials (CP reduction occurred before the initiation of the metal reduction processes). Finally, the flat galvanostatic curve, observed in the Cu^{2+} case at potentials corresponding to the hydrogen reduction reaction in the acid copper cations solution (Fig. 7a), indicated that small partial currents were initially consumed for metal nucleation and growth, and this process was significantly inhibited.

Similar effects were observed when using silver anion complexes (Ag–thiosulfate and Ag–EDTA) instead of silver cations (Fig. 7b) [90]. The sharp maximum observed in the

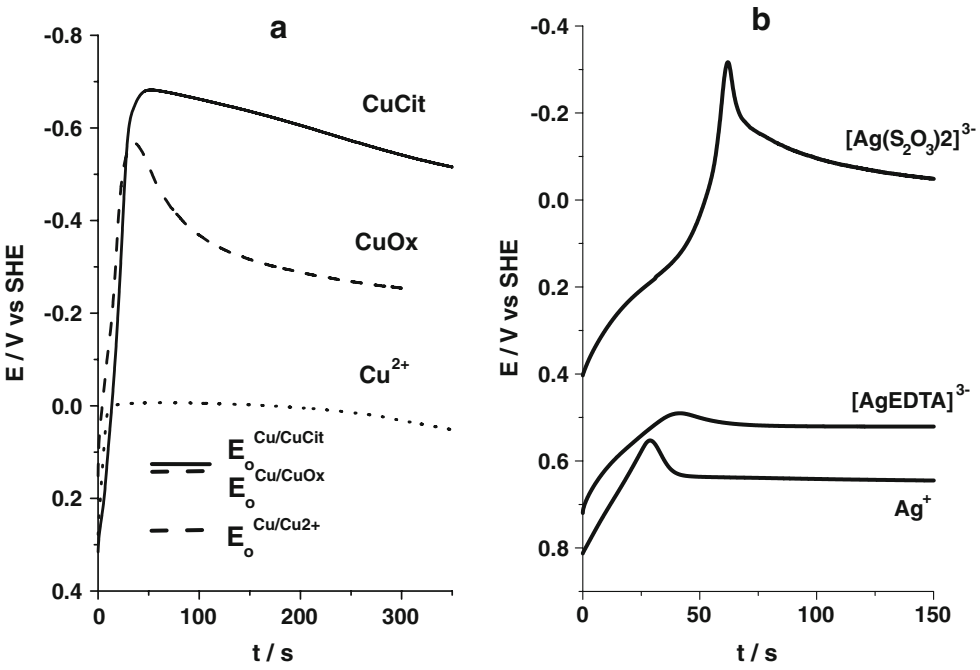

Fig. 7 Galvanostatic transients obtained at a PANI layer in different copper (**a**) and silver (**b**) ion containing solutions; j=−0.18 mAcm^{-2}, Q_{red}=20 mCcm^{-2} for copper and j=−0.2 mAcm^{-2}, Q_{red}=18 mCcm^{-2} for silver. The OCP potentials of bulk copper in the different copper ion containing solutions is denoted by the corresponding E_o

Ag–thiosulfate case indicated metal nucleation and growth starting after additional reduction (shoulder in the galvanostatic curve observed in the first 50 s) of the PANI layer. Silver electroreduction in the cation-containing solution occurred very close to equilibrium ($E_0^{Ag/Ag^+} = 0.68$ V) giving evidence for an easy metal nucleation and growth process. The galvanostatic curve obtained in the Ag–EDTA case with initial shoulder and rounded maximum showed the parallel involvement of PANI and metal ions reduction. These qualitative observations were supported by measurements on PANI-coated electrodes in corresponding supporting electrolytes in the absence of the metal anion complexes allowing to follow the reductive behavior of the PANI layers alone [90].

The results obtained for both Cu/PANI and Ag/PANI systems have shown that the various metal anion complexes give rise to the shift of the potential window for metal deposition in the negative direction; thus, allowing, in some cases (e.g., Cu–citrate and Ag–thiosulfate), to separate the polymer and the metal ions reduction process. In this situation, metal nucleation and growth occurred at reduced PANI layers and resulted in both cases in the formation of small numbers (10^6 cm^{-2}) of large (micrometer-sized) crystals on the polymer surface (e.g., Fig. 8a). In some cases, e.g., copper electroreduction in Cu–oxalate solution, both metal ion and CP reduction proceeded in parallel; and in this situation, a homogeneous surface distribution of a large number (10^8 cm^{-2}) of small (150 nm) copper particles

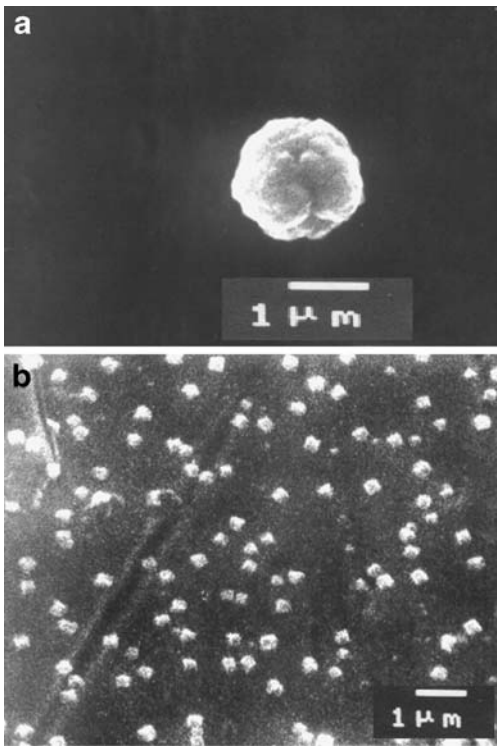

Fig. 8 SEM of copper crystals obtained after galvanostatic deposition using Cu–thiosulfate (**a**) and (**b**) Cu–oxalate solutions

was obtained (Fig. 8b). Based on our investigations carried out with PANI layers, it was difficult to identify the role of the various ligands for the oxidation state of the CP layer, the transport of the metal complex anions in the PANI layers, and finally, for the growth shape of the metal crystals. Further experiments, preferably involving CP layers with pH-independent oxidation state and conductivity, are needed to elucidate these points.

Metal stabilization in CPs as a preliminary step for metal electrocrystallization

Studies on metal electrodeposition in CP-coated electrodes have shown that the electrochemical reduction of metal ions does not always result in crystallization alone but also in the chemical stabilization of metal species in the volume of the polymer layer. This effect and, in general, metal/CP interactions were observed in several systems [91, 92, 103, 106, 120, 139–152] (see Table 1). In several cases [139–149], evidence was obtained for the interaction of partially reduced metal ions, e.g., Cu(I) or Au(I), to specific (nitrogen or sulfur) sites of the polymer chains, resulting in the formation of metal/polymer complexes. In our recent investigations on copper electroreduction in PEDOT [91, 92], it was shown that by driving the process at constant low overpotential, it became possible to introduce reduced copper atoms in the polymer layers without building copper crystals. The copper atoms were reversibly oxidized to Cu (I) ions, the latter remaining captured inside the PEDOT layer. To our knowledge, the incorporation of metal species (ions and single atoms) in CPs was not intentionally used as a starting point for the electrocrystallization of metal particles.

Such an attempt was carried out in the study on the role of the PEDOT-stabilized Cu species for the copper electrocrystallization process [93]. In this investigation, one-step (direct crystallization at high overpotential) and two-step (stabilization at low overpotential and subsequent crystallization at high overpotential) experiments were performed. Figure 9 shows the microscopic pictures of the surface of PEDOT specimens obtained after directly applying a crystallization overpotential (η=70 mV for 25 s) and after a two-step electroreduction experiment (η=30 mV for 2 h and η=70 mV for 20 s). It is evident that the presence of stabilized species favors the copper electrocrystallization process. It is difficult to specify whether the stabilized copper atoms act directly as additional active sites for copper crystallization or rather affect the polymer electronic structure. Nevertheless, it is clear that, in all cases of metal stabilization in CPs, this effect could be used for modifying the polymer structure from both chemical and electronic point of views and provides an additional, still unexplored tool for influencing the characteristics of the deposited metal particles.

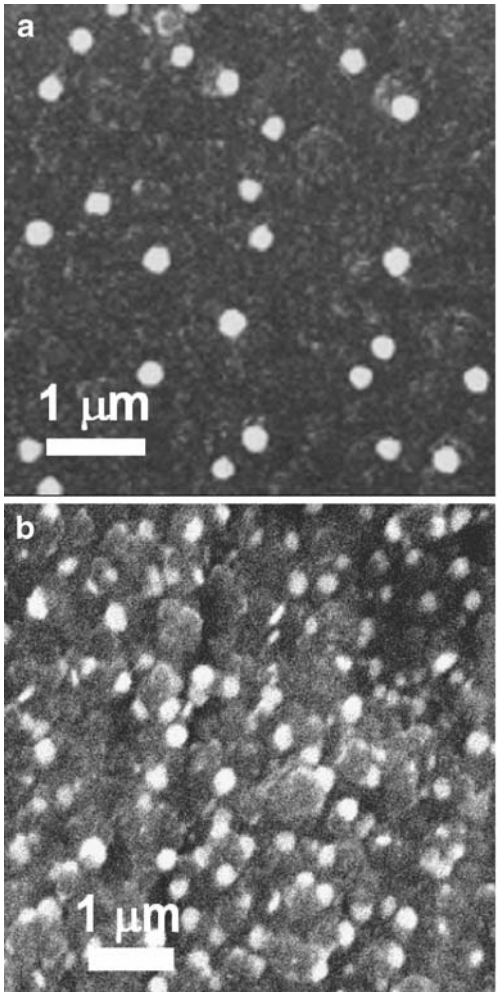

Fig. 9 SEM of Cu–PEDOT specimens obtained after one-step (**a**) and two-step (**b**) potentiostatic experiments

Metal particles electrodeposition method

In general, there are three basic approaches for electrodepositing metal particles in CP layers:

1. *Polymer electrosynthesis in the presence of metal ions*. This may result in the direct deposition of the metal particles during synthesis [22, 47, 56] or complex metal anions entrapment during the polymer electrosynthesis. In the latter case, metal particles are formed in a subsequent potentiostatic reduction step [21, 24, 36, 41].
2. *Polymer layer electrosynthesis (in the absence of metal ions) followed by metal electrodeposition*. All usual experimental techniques for producing metal deposits on inert conducting substrates, e.g., potentiostatic, galvanostatic, potentiodynamic, and also pulse techniques, have been applied for the second metal deposition step.
3. *Incorporation of chemically synthesized colloidal metal particles in the course of polymer layer electrosynthesis* [24, 36, 153–156] (see Table 1). This approach provides the advantage to incorporate nanoparticles with predefined characteristics.

A comparison between the results obtained by the first two approaches mentioned above present the investigations on Pd deposition in PANI [47] and Pt, Rh, Ru, Ir, and Pd deposition in PPY [21, 24, 41, 45]. The first approach resulted in metal particles with three-dimensional homogeneous distribution inside the polymer layer [21, 24, 41]. Increased amount of metal near the polymer/metal substrate interface was observed in the Pd/PANI case [47]. The second approach, carried out on oxidized CP layers, typically resulted in preferential deposition on the outer polymer surface [21, 24, 41, 47] in accordance with the already discussed case of Cu deposition in oxidized PANI. Only in the case of thin (about 0.1 μm) PPY layers no difference in the depth profile of the distributed Pd particles was observed [45].

As far as the different techniques for metal electrodeposition within the second approach are concerned, the galvanostatic approach [41, 83, 84, 86–88, 91, 94] provides the possibility to get a qualitative insight into the participation of parallel reduction processes. At the same time, in galvanostatic experiments, the growth of the metal particles occurs under varying overpotential and may result in broader size distributions and various growth shapes of the metal crystals. Potentiostatic deposition (e.g., [46, 49, 51, 53, 84, 85, 87, 89, 92, 93]), on the other hand, allows driving the electrochemical growth of the metal crystals at constant overpotential and offers the possibility for initiating instantaneous nucleation. This would result in narrower size distributions of the metal particles and in low overpotential experiments in equilibrium-shaped crystals. Another advantage of the potentiostatic technique is that it provides, in the rule, additional information on the kinetics of the metal nucleation and growth. The theoretical modeling of potentiostatic current transients obtained in the course of metal electrocrystallization in CPs encounters, however, specific difficulties due to the fact that the usually addressed models [157–158] refer to nucleation on a flat conducting substrate and to electrochemical growth involving a simple one-step electron transfer for the reduction of metal cations to metal atoms. Thus, if the internal polymer surface of the layer becomes involved in the metal particles nucleation and growth and/or additional reduction processes (e.g., CP reduction or metal ions reduction resulting in metal-CP stabilization) proceed in parallel with the metal ions reduction involved in the electrocrystallization process, the applications of these models is rather questionable. Another effect, which may compromise the adequate modeling of experimental current transients, is the possible interference of electroless precipitation occurring before or in the initial

stage of the electrodeposition process (see the "Electroless precipitation of metals in CPs" section). Nevertheless, for very thin CP layers, the modeling of potentiostatic current transients by existing model equations for the current seems to be justified [46, 53]. For thicker layers, the parallel CP reduction could be taken into account by making reference measurements in the absence of metal ions and correcting the metal electrocrystallization current transients [51, 89] or by fixing the initial oxidation state of the CP layer through appropriate potentiostatic preconditioning [85, 87]. These approaches resulted in reasonable modeling of the current transients of silver and copper electrocrystallization in PANI [84, 87, 89].

The various attempts to involve potentiostatic [29–31, 39, 48, 62, 68] or galvanostatic [34, 56] pulse methods for metal electrocrystallization in presynthesized CP layers turned out to be appropriate for keeping the CP layer in the oxidized state or limiting the growth stage and thus keeping the size of the metal particles in the nanoscale. The comparison of potentiostatic and pulse potentiostatic technique for Pt electrodeposition in PANI [30] showed a preferential deposition of the metallic phase at the polymer surface for the potentiostatic technique against an efficient dispersion of the Pt in the polymer matrix, obtained by the pulse technique.

Finally, another interesting method for depositing nanoparticles in CPs (not fitting within the three approaches mentioned above) was recently suggested for the Au/PANI system by Smith et al. [60, 61]. This approach involved the deposition of a thin, sacrificial Au layer on a Pt substrate, electropolymerization of PANI on the Au-plated substrate, gold oxidation in chloride solution, and finally, reduction of the $AuCl^{4-}$ complexes entrapped in the PANI structure. Thus, gold/PANI free-standing composite films were produced [60, 61].

Electroless precipitation of metals in CPs

Electroless precipitation in conducting polymer materials is based on the intrinsic ability of CPs to occupy different interconvertible oxidation states and couples following reactions:

$$Me^{n+} + ne^- \rightarrow Me^0 \quad (1)$$

$$CP^{m+} \rightarrow CP^{(m+n)+} + ne^- \quad (2)$$

where n is the number of electrons exchanged for reducing a single metal ion and m denotes the extent of initial oxidation of the CP material.

This process proceeds in both acidic [96–99, 101, 104, 106, 109, 112–114, 117, 118, 120, 121, 123, 125] and neutral aqueous solutions [103, 113, 114, 122–126] and was also investigated for CP materials dissolved in organic solvents [105, 110, 111, 113, 115, 116, 125]. In acidic solutions, electroless precipitation in PANI and PPY layers proceeds as a self-sustained process due to the initial deprotonation (and oxidation) and subsequent spontaneous reprotonation (and reduction) of the nitrogen sites in these polymers (see, e.g., [96, 97, 101]). This process was extensively studied in the case of Pd precipitation in PANI [104, 106, 107, 110] and POMA [121].

Electroless precipitation was used as a tool for producing metal deposit in supported CP layers, films, and membranes in a number of cases [50, 90, 95, 101–103, 112, 116–120, 122, 123, 126, 127] (see Table 1). These investigations give insight into the role of several factors influencing the electroless precipitation process:

Initial oxidation state of the CP layers

The initial oxidation state of the CP layer, which may be modified either through chemical or electrochemical pretreatment, is of primer importance for the occurrence and driving force of the electroless precipitation process. There are several studies addressing the electroless metal precipitation in chemically reduced CPs [106, 109, 112, 116, 120]. Comparative studies of metal electroless precipitation by using different oxidation states of PANI and PPY films showed effective electroless deposition of Pd in fully reduced leucoemeraldine PANI [109] and fully reduced PPY [112].

Electrochemical reductive pretreatment of supported CP layers in the absence of metal ions and subsequent dipping in the metal-plating solution was carried out in several cases [4, 50, 90, 95, 103, 118]. In this way, the precipitation process was driven by a larger potential difference between the initial dipping OCP and the equilibrium potential of the specific metal in the corresponding metal ion plating solution. In our studies on Ag electroless precipitation in PANI [90], this approach provided the opportunity for the formation of homogeneously distributed metal nanoparticles on the polymer surface within several minutes. It was shown that the reduction charge of the polymer layer and the dipping time are suitable parameters providing effective control over the amount of precipitated metal.

Although the acidity of the plating electrolyte is also influencing the oxidation state of the CP materials such as PANI and PPY, little attention has been so far paid to the role of this parameter for the characteristics of the precipitated metal particles. In the case of PANI and PPY, silver recovery was found to proceed more effectively in near neutral than in strongly acidic solutions [123]. Based on comparative investigations in the PANI/gold system by using PANI exchanged with HBF_4 or CHOOH, Smith et al.

[117] draw attention to the strength of the acids initially incorporated in the CP layer for the characteristics of the metal deposit. In the same line are the recent investigations of Wang et al. [127], demonstrating the effect of the doping anion, available in the CP layer, on the microscopic picture of the Ag deposit in PANI. A large variety of growth shapes and sizes of the precipitated silver crystals was observed by doping PANI layers with hydrochloric, mandelic, citric, *p*-toluenesulfonic, trifluroacetic, and phosphoric acids [127]. Nevertheless, systematic studies are needed to understand the role of the acidity of the plating electrolyte and type of doping anion and employ these factors as a tool for influencing the characteristics of the metal deposit.

Role of the surface morphology of the CP layers

PANI layers with different surface structures (produced through various potentiodynamic polymerization regimes) were used for the electroless precipitation of Pd by Mourato et al. [118]. It was found that, for the more compact PANI surface, Pd clusters with an average size of 20 nm and also larger clusters with size distribution (80–200 nm) were precipitated. For the more porous PANI structure, smaller clusters (15 nm) with very narrow size distribution were observed together with larger clusters in the 100- to 200-nm scale. With this exception, the role of the surface morphology of the CP layers for electroless metal precipitation was not addressed.

Concentration of the metal ions plating solution

The concentration of the metal-plating solution is a useful tool allowing to switch the rate-determining step of the precipitation reaction between transport limitations of the metal ions in the solution (for low concentrations) and CP-based kinetic limitations (for high concentrations) [126]. A clear illustration of this effect provided the Ag/PANI system [90]. Using low metal ions concentration (0.2 mM) and relatively short dipping times allowed fixing the amount of deposited silver, irrespective of the PANI layers redox charge [90]. On the other hand, by keeping the amount of deposited Ag one and the same, and using different metal ions concentrations (2 mM and 10 mM), it was possible to affect the number density and size distribution of the metal particles. At the higher concentration, a lower number of almost equally sized Ag particles (Fig. 10a) was formed, a situation corresponding to the instantaneous nucleation of the metal particles. Reducing the concentration of the metal anion species present in the solution slowed down the metal nucleation and growth process and resulted in the appearance of a higher number of Ag particles with broader size distribution (Fig. 10b).

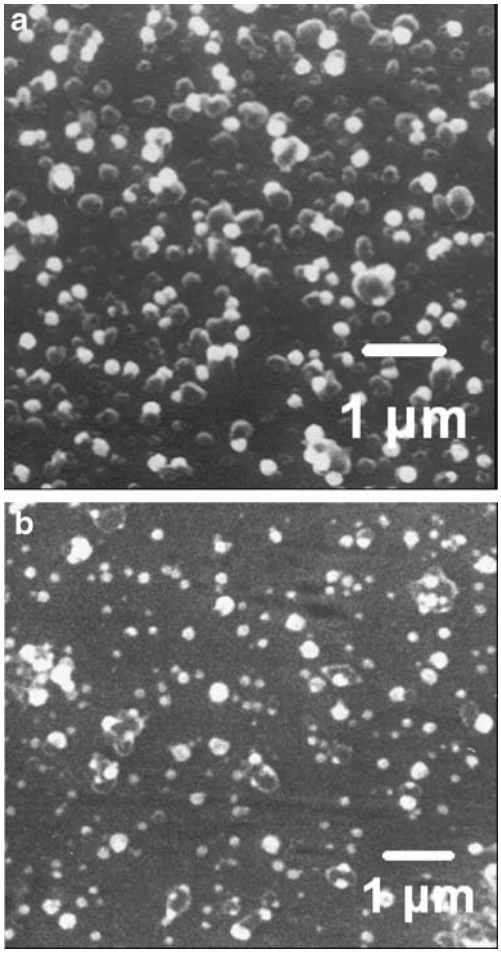

Fig. 10 SEM of Ag/PANI specimens obtained by electroless precipitation in Ag–EDTA solution with two concentrations: **a** 10 mM and **b** 2 mM; Q_{red}=42 mCcm^{-2}

Comparison between electroless and electrodriven metal particles deposition

To our knowledge, there are no relevant comparative studies of the metal deposit obtained through electrodriven deposition and electroless precipitation under fully comparable conditions. A comparative investigation, carried out in the case of Pd deposition in PANI [50], showed a larger number of equally sized crystals for the electrodeposition case against a smaller particle number with broader size distribution for the electroless precipitation case. However, these results were obtained by using palladium solutions with different acidity, concentration, and counter ion; and thus, it is difficult to identify a single factor responsible for this result.

In general, the basic advantage of metal electroless precipitation over metal electrodeposition seems to be the possibility to eliminate the role of structural microdefects available in the CP layer. The most favorable sites for metal particles precipitation are those where the polymer structure becomes readily oxidized. Thus, the polymer morphology

is again of primer importance, but instead of the defects, the active sites for nucleation are most probably polymer chains with higher extent of conjugation and order. Further investigations are needed to identify the active sites for nucleation for electrodriven and electroless metal deposition and relate them to the local morphology and conductivity characteristics of the CP layers.

Conclusions

The discussion of the results on metal electrodeposition in conducting polymer layers presented in this paper points out to the following specific aspects of this process:

1. The electroreduction of metal ions in conducting polymer layers is often accompanied by CPs intrinsic reductive processes, providing, in general, a situation quite different from the electrodeposition of metal particles on inert substrates. The overlapping of potential windows corresponding to the different reduction processes becomes easily discernible by means of galvanostatic experiments. In this specific situation, it is often difficult to carry out kinetic studies (e.g., through potentiostatic experiments) on electrochemical nucleation and growth. In many cases, the application of theoretical models for the initial stages of metal electrocrystallization for the interpretation of experimentally obtained current transients is complicated due to the interference of parallel electrochemical processes and the involvement of the internal polymer structure in the nucleation and growth process.
2. In the case of electrodriven deposition, the conductivity and morphology characteristics (surface homogeneity, amount of defects, density, and roughness of the polymer structure) of the CP layers determine, in combination, the location of the deposited metal particles. In general, the larger the CP surface inhomogeneity and roughness, the larger the role of the underlying substrate for the metal nucleation and growth process may become.
3. The application of various techniques for the metal particles electrodeposition in morphologically homogeneous CP layers may be used for influencing the location of the metal deposit. Polymer electrosynthesis in the presence of metal ions results in the rule in metal particles distributed in the bulk of the CP layer whereas electrodeposition carried out in a separate step, after CP synthesis, provides usually preferential deposition at the polymer/solution interface. Pulse metal electrodeposition methods are prospective tools to be further used for influencing the location of the metal deposit in readily polymerized CP layers.
4. The involvement of various metal anion complexes, instead of the corresponding cations, in metal particles electrodeposition in CP layers opens a new and yet little explored approach for influencing the characteristics of the metal deposit. Further experimentation is needed to understand how the different ligands interact with the polymer matrix, influence the metal ions transport through the polymer structure, and affect the metal nucleation and growth process.
5. In the case of electroless metal precipitation, the local intrinsic characteristics (extent of oxidation and ordering of the polymer chains) of the polymer surface are of major importance whereas the underlying electrode substrates is not involved in the process. Bearing in mind the possibility for electrochemical control over the amount and size distribution of the precipitated metal particles, electroless precipitation seems to be a suitable alternative to the conventional electrodriven electrocrystallization, especially for practical applications. Several factors, such as the role of surface morphology, conductivity of the CP layers, acidity, type of the compensating anion or metal ligand, and concentration of the plating solutions, need to be studied in further details to achieve better understanding and control over the process. Combining of electroless precipitation and electrodriven deposition opens new still unexplored prospects for metal modification of CPs. Based on such an approach, first attempts for bimetal (Cu and Pd) modification of PEDOT layers were recently communicated [95].

Finally, it is my hope that the discussion of results and specific aspects outlined in this paper will provoke further studies on metal deposition in conducting polymers coatings and help in eventually solving practical problems related to the distribution of large amounts of small metal particles in CP layers.

Acknowledgements I am grateful to my colleague M. Ilieva and my students—D. Borissov, S. Ivanov, L. Komsiyska, and A. Stoyanova—for their motivated work and contribution to the clarification of different aspects of our studies. The investigations are supported by the Bulgarian Ministry of Education and Science under contract VUH-307 and the FP 6 European Project NANOPHEN (INCO-CT-2005-016696).

References

1. Tourillon G, Garnier F (1984) J Phys Chem 88:5281
2. Chandler GK, Pletcher D (1986) J Appl Electrochem 16:62
3. Kost K, Bartak D, Kazee B, Kuwana Th (1988) Anal Chem 60:2379
4. Holdcroft S, Funt BL (1988) J Electroanal Chem 240:89
5. Vork FTA, Janssen LJJ, Barendrecht E (1986) Electrochim Acta 31:1569

6. Esteban PO, Leger JM, Lamy C, Genies E (1989) J Appl Electrochem 19:462
7. Gholamian M, Contractor AQ (1990) J Electroanal Chem 289:69
8. Strike DJ, De Rooij NF, Koudelka-Hep M (1992) J Appl Electrochem 22:922
9. Ulmann M, Kostecki R, Augustinsky J, Strike DJ, Koudelka-Hep M (1992) Chimia 46:138
10. Swathirajan S, Mikahil YM (1992) J Electrochem Soc 139:2105
11. Hable C, Wrighton MS (1993) Langmuir 9:3284
12. Kostecki R, Ulmann M, Augustynski J, Strike DJ, Koudelka-Hep M (1993) J Phys Chem 97:8113
13. Grzeszczuk M (1994) Electrochim Acta 39:1809
14. Moutet JC, Ouennoughi Y, Ourari A, Hamar-Thibault S (1995) Electrochim Acta 40:1827
15. Lai EKW, Beattie PD, Holdcroft S (1997) Synth Met 84:87
16. Ficicioglu F, Kadirgan F (1998) J Electroanal Chem 451:95
17. Croissant MJ, Napporn T, Leger JM, Lamy C (1998) Electrochim Acta 43:2447
18. Yang CH, Wen TC (1998) Electrochim Acta 44:207
19. Kelaidopoulou A, Abelidou E, Papoutsis A, Polychroniadis EK, Kokkinidis G (1998) J Appl Electrochem 28:1101
20. Del Valle MA, Diaz FR, Bodini ME, Pizarro T, Cordova R, Gomez H, Schrebler R (1998) J Appl Electrochem 28:943
21. Hepel M (1998) J Electrochem Soc 145:124
22. Maksimov YM, Podlovchenko BI, Gladysheva TD, Kolyadko EA (1999) Russ J Electrochem 35:1225
23. Coutanceau C, Croissant MJ, Napporn T, Lamy C (2000) Electrochim Acta 46:579
24. Bouzek K, Mangold KM, Juettner K (2000) Electrochim Acta 46:661
25. Castro-Luna AM (2000) J Appl Electrochem 30:1137
26. Mikahylova AA, Molodkina EB, Khazova OA, Bagotzky VS (2001) J Electroanal Chem 509:119
27. Kitani A, Akashi T, Sugimoto K, Ito S (2001) Synth Met 121:1301
28. Ocon P, Herrasti P, Rojas S (2001) Polymer 42:2439
29. Kessler T, Castro Luna AM (2002) J Appl Electrochem 32:825
30. Hu CC, Chen E, Lin JY (2002) Electrochim Acta 47:2741
31. Kessler T, Castro Luna AM (2003) J Solid State Electrochem 7:593
32. Niu L, Li Q, Wei F, Chen X, Wang H (2003) Synth Met 139:271
33. Niu L, Li Q, Wei F, Chen X, Wang H (2003) J Electroanal Chem 544:121
34. Zhou HH, Jiao SQ, Chen JH, Wei WZ, Kuang JF (2004) J Appl Electrochem 34:455
35. Mascaro LH, Goncalves D, Bulhoes LOS (2004) Thin Solid Films 461:243
36. Juttner K, Mangold KM, Lange M, Bouzek K (2004) Russ J Electrochem 40:317
37. Biallozor S, Kupniewska A, Jasulajtene V (2004) Bull Electrochem 20:231
38. Biallozor S, Kupniewska A (2004) Bull Electrochem 20:241
39. Niu L, Li Q, Wei F, Wu S, Liu P, Cao X (2005) J Electroanal Chem 578:331
40. Wang G, Li L, Li JH, Xu BQ (2005) Carbon 43:2579
41. Trueba M, Trasatti SP, Trasatti S (2006) Mater Chem Phys 98:165
42. Kuo CW, Huang LM, Wen TC, Gopalan A (2006) J Power Sources 160:65
43. Kinyanjui JM, Wijeratne NR, Hanks J, Hatchett DW (2006) Electrochim Acta 51:2825
44. Yassar A, Roncali J, Garnier F (1988) J Electroanal Chem 255:53
45. De Oliveira IMF, Moutet JC, Hamar-Thibault S (1992) J Mater Chem 2:167
46. Leone A, Marino W, Scharifker B (1992) J Electrochem Soc 139:438
47. Li HS, Josowicz M, Baer DR, Engelhardt M, Janata J (1995) J Electrochem Soc 142:798
48. Torsi L, Pazzuto M, Siciliano P, Rella R, Sabbatini L, Valli L, Zambonin PG (1998) Sens Actuators B Chem 48:362
49. Frydrychewicz A, Vassilev SYu, Tsirlina GA, Jackowska K (2005) Electrochim Acta 50:1885
50. Mourato A, Wong SM, Siegenthaler H, Abrantes LM (2006) J Solid State Electrochem 10:140
51. Mourato A, Correia JP, Siegenthaler H, Abrantes LM (2007) Electrochim Acta 53:664
52. Lee JY, Tan TC (1990) J Electrochem Soc 137:1402
53. Tsakova V, Milchev A (1991) Electrochim Acta 36:1151
54. Tian ZQ, Lian YZ, Wang JQ, Li WH (1991) J Electroanal Chem 308:357
55. Hernandez N, Ortega JM, Choy M, Ortiz R (2001) J Electroanal Chem 515:123
56. Zhou HH, Ning XH, Li SL, Chen JH, Kuang YF (2006) Thin Solid Films 510:164
57. Hatchett DW, Josowicz M, Janata J, Baer DR (1999) Chem Mater 11:2989
58. Hwang BJ, Santhanam R, Lin YL (2003) Electronalysis 15:1667
59. Kinyanjui JM, Hanks J, Hatchet DW, Smith A, Josowicz M (2004) J Electrochem Soc 151:D113
60. Smith JA, Josowicz M, Janata J (2005) Phys Chem Chem Phys 7:3614
61. Smith JA, Josowicz M, Engelhard M, Baer DR, Janata J (2005) Phys Chem Chem Phys 7:3619
62. Wang Z, Yuan J, Li M, Han D, Zhang Y, Shen Y, Niu L, Ivaska A (2007) J Electroanal Chem 599:121
63. Leeuw DM, Kraakman PA, Bongaerts PFG, Mutsaers CMJ, Klaassen DBM (1994) Synth Met 66:263
64. Nichols RJ, Schroer, Mayer H (1995) Electrochim Acta 40:1479
65. Abrantes LM, Correia JP (1996) Electrochim Acta 42:1747
66. Jovic VD, Trisovic T, Jovic BM, Vojnovic M (1996) J Electroanal Chem 408:149
67. Hepel M, Chen YM, Stephenson R (1996) J Electrochem Soc 143:498
68. Guascito MR, Boffi P, Malitesta C, Sabbatini L, Zambonin PG (1996) Mater Chem Phys 44:17
69. Zouaoui A, Stephan O, Carrier M, Moutet JC (1999) J Electroanal Chem 474:113
70. Ortega JM (2000) Thin Solid Films 360:159
71. Martinot L, Leroy D, Zhan H, Licour C, Jerome C, Chapelle G, Calberg C, Jerome R (2000) J Mater Chem 10:729
72. Cioffi N, Torsi L, Losito I, Di Franco C, De Bari I, Chiavarone L, Scamarcio G, Tsakova V, Sabbatini L, Zambonin PG (2001) J Mater Chem 11:1434
73. Liu YC, Yang KH, Ger MD (2002) Synth Met 126:337
74. Sarkar DK, Zhou XJ, Tannous A, Louie M, Leung KT (2003) Solid State Commun 125:365
75. Zhou XJ, Harmer AJ, Heinig NF, Leung KT (2004) Langmuir 20:5109
76. Otero TF, Costa SO, Ariza MJ, Marquez M (2005) J Mater Chem 15:1662
77. Abrantes LM, Correia JP (1998) Surf Coat Technol 107:142
78. Abrantes LM, Correia JP (1998) Port Electrochim Acta 16:85
79. Abrantes LM, Correia JP (2000) Electrochim Acta 45:4179
80. Zaoui A, Stephan O, Ourari A, Moutet JC (2000) Electrochim Acta 46:49
81. Watanabe N, Morais J, Accione SBB, Morrone A, Schmidt JE, Alves MCM (2004) J Phys Chem 108:4013
82. Tsakova V, Borissov D (2000) Electrochem Commun 2:511
83. Tsakova V, Borissov D, Ivanov S (2001) Electrochem Commun 3:312
84. Tsakova V, Borissov D, Ranguelov B, Stromberg Ch, Schultze JW (2001) Electrochim Acta 46:4213
85. Tsakova V, Winkels S, Schultze JW (2001) J Electroanal Chem 500:574

86. Ivanov S, Tsakova V (2002) J Appl Electrochem 32:701
87. Ivanov S, Tsakova V (2002) J Appl Electrochem 32:709
88. Ivanov S, Mokreva P, Tsakova V, Terlemezyan L (2003) Thin Solid Films 441:44
89. Ivanov S, Tsakova V (2004) Electrochim Acta 49:913
90. Ivanov S, Tsakova V (2005) Electrochim Acta 50:5616
91. Ilieva M, Tsakova V (2004) Synth Met 141:281
92. Ilieva M, Tsakova V (2004) Synth Met 141:287
93. Ilieva M, Tsakova V (2005) Electrochim Acta 50:1669
94. Komsiyska L, Tsacheva Ts, Tsakova V (2005) Thin Solid Films 493:88
95. Ilieva M, Tsakova V, Erfurth W (2006) Electrochim Acta 52:816
96. Kang ET, Ting YP, Neoh KG, Tan KL (1993) Polymer 34:4494
97. Ting YP, Neoh KG, Kang ET, Tan KL (1994) J Chem Technol Biotechnol 59:31
98. Kang ET, Ting YP, Neoh KG, Tan KL (1995) Synth Met 69:477
99. Pickup NL, Shapiro JS, Wong DKY (1998) Anal Chim Acta 364:41
100. Abrantes LM, Cascalheira AC, Savic M (1999) Port Electrochim Acta 17:157
101. Abrantes LM, Correia JP (1995) Mat Sci Forum 191:235
102. Langmaier J, Janata J (1992) Anal Chem 64:523
103. Zhang AQ, Cui CQ, Lee JY, Loh FC (1995) J Electrochem Soc 142:1097
104. Hasik M, Derlinkiewicz A, Choczynski M, Quillard S, Pron A (1997) Synth Met 84:93
105. Lebedev MY, Lauritzen MV, Curzon AE, Holdcroft S (1998) Chem Mater 10:156
106. Derlinkiewicz A, Hasik M, Choczynski M (1998) Mater Res Bull 33:739
107. Derlinkiewicz A, Hasik M, Kloc M (1999) Synth Met 102:1307
108. Josowicz M, Li HS, Domansky K, Baer DR (1999) Electroanalysis 11:774
109. Ma ZH, Tan KL, Kang ET (2000) Synth Met 114:17
110. Derlinkiewicz A, Hasik M, Kloc M (2000) Catal Letters 64:41
111. Hasik M, Drelinkiewicz A, Wenda E (2001) Synth Met 119:335
112. Lim VWL, Kang ET, Neoh KG (2001) Synth Met 123:107
113. Wang J, Neoh KG, Kang ET (2001) J Colloid Interface Sci 239:78
114. Khan MA, Perruchot C, Armes SP, Randall DP (2001) J Mater Chem 11:2631
115. Hasik M, Derlinkiewicz A, Wenda E (2001) Synth Met 119:335
116. Lee M, Kim BW, Nam JD, Lee Y, Son Y, Seo SJ, Lee Y (2003) Mol Cryst Liq Cryst 407:397
117. Smith JA, Josowicz M, Janata J (2003) J Electrochem Soc 150:E384
118. Mourato A, Viana AS, Correia JP, Siegenthaler H, Abrantes LM (2004) Electrochim Acta 49:2249
119. Kim BY, Cho MS, Kim YS, Son Y, Lee Y (2005) Synth Met 153:149
120. Hasik M, Wenda E, Paluskiewicz C, Bernasik A, Camra J (2004) Synth Met 143:341
121. Derlinkiewicz A, Hasik M, Sobczak JW, Sobczak E, Bernasik A, Bielanska E (2005) Mater Res Bull 40:869
122. Jovanovic VM, Terzic S, Dekanski A (2005) J Serb Chem Soc 70:41
123. Dimeska R, Murray PS, Ralph SF, Wallace GG (2006) Polymer 47:4520
124. Sofiane B, Didier H, Laurent LP (2006) Electrochim Acta 52:62
125. O'Mullane AP, Dale SE, Day TM, Wilson NR, Macpherson JV, Unwin PR (2006) J Solid State Electrochem 10:792
126. Ocypa M, Ptasinska M, Michalska A, Maksymiuk K, Hall EAH (2006) J Electroanal Chem 596:157
127. Wang HL, Li W, Jia QX, Akhadov E (2007) Chem Mater 19:520
128. Tsakova V, Milchev A (1991) Electrochim Acta 36:1579
129. Tsakova V, Milchev A, Schultze JW (1993) J Electroanal Chem 346:85
130. Tsakova V, Winkels S, Schultze JW (2000) Electrochim Acta 46:759
131. Stromberg C, Tsakova V, Schultze JW (2003) J Electroanal Chem 547:125
132. Volfkovich YM, Bagotzky VS, Zolotova TK, Pisarevskaya EY (1996) Electrochim Acta 41:1905
133. Vikarchuk AA, Volenko AP, Gamburg YuD, Bondarenko SA (2004) Russ J Electrochem 40:180
134. Vikarchuk AA, Volenko AP (2005) Phys Solid State 47:352
135. Kashchiev D (1975) Thin Solid Films 29:193
136. Baraboshkin AN (1976) Elektrokristallizacija metallov iz razplavlennih solei. Nauka, Moskva
137. Milchev A, Montenegro I (1992) J Electroanal Chem 333:92
138. Hasse U, Fletcher S, Scholz F (2006) J Solid State Electrochem 10:833
139. Rau J, Lee J, Chen S (1996) Synth Met 79:69
140. Inoue MB, Nebesny KW, Fernando Q (1990) Synth Met 38:205
141. Liu YC, Hwang BJ (1999) Thin Solid Films 339:233
142. Liu YC, Hwang BJ (2001) J Electroanal Chem 501:100
143. Liu Y, Yang K, Ger M (2002) Synth Met 126:337
144. Tourillon G, Dartyge E, Dexpert H, Fontaine A, Jucha A, Lagarde P, Sayers DE (1984) J Electroanal Chem 178:357
145. Tourillon G, Dartyge E, Dexpert H, Fontaine A, Jucha A, Lagarde P, Sayers DE (1985) Surf Sci 156:536
146. Tourillon G, Dartyge E, Fontaine A, Jucha A (1986) Phys Rev Lett 57:603
147. Gourier D, Tourillon G (1986) J Phys Chem 90:5561
148. Guay D, Tourillon G, Fontaine A (1990) Faraday Discuss Chem Soc 89:41
149. Guay D, Tourillon G, Dartyge E, Fontaine A, Tolentino H (1991) J Electrochem Soc 138:399
150. Sobczak JW, Sobczak E, Kosinski A, Bilinski A (2001) J Alloys Comp 328:132
151. Park JE, Park SG, Koukitu A, Hatozaki O, Oyama N (2004) Synth Met 141:265
152. Posdorfer J, Wessling B (2001) Synth Met 119:363
153. Bose CSC, Rajeshwar K (1992) J Electroanal Chem 333:235
154. Chen CC, Bose CSC, Rajeshwar K (1993) J Electroanal Chem 350:161
155. Cioffi N, Torsi L, Sabbatini L, Zambonin PG, Bleve-Zacheo T (2000) J Electroanal Chem 488:42
156. Grzeszczuk M, Poks P (2000) Electrochim Acta 45:4171
157. Harrison JA, Thirsk HR (1971) In: Bard AJ (ed) Electroanalytical chemistry, vol 5. Marcel Dekker, New York, p 67
158. Budevski E, Staikov G, Lorenz WJ (1996) Electrochemical phase formation—an introduction to the initial stages of metal deposition. VCH, Weinheim
159. Ko JM, Park DY, Myung NV, Chung JS, Nobe K (2002) Synth Met 128:47